Brain PET in Suspected Dementia: Patterns of Altered FDG Metabolism[1]

Richard K. J. Brown, MD
Nicolaas I. Bohnen, MD, PhD
Ka Kit Wong, MBBS
Satoshi Minoshima, MD, PhD
Kirk A. Frey, MD, PhD

Abbreviations: CAD = computer-assisted diagnosis, DLB = dementia with Lewy bodies, FDG = 2-[fluorine-18]fluoro-2-deoxy-D-glucose, FTD = frontotemporal dementia, MCI = mild cognitive impairment, PCA = posterior cerebral atrophy, SPM = statistical parametric mapping, SSP = stereotactic surface projection, 3D = three-dimensional

RadioGraphics 2014; 34:684–701

Published online 10.1148/rg.343135065

Content Codes: MI NM NR

[1]From the Department of Nuclear Medicine/Radiology, University of Michigan, 1500 E Medical Center Dr, B1 G505, Ann Arbor, MI 48109-5028 (R.K.J.B., N.I.B., K.K.W., K.A.F.); Neurology Service and Geriatric Research, Education and Clinical Center (GRECC) (N.I.B.) and Department of Nuclear Medicine (K.K.W.), VA Ann Arbor Healthcare System, Ann Arbor, Mich; and Department of Radiology, University of Washington, Seattle, Wash (S.M.). Received April 17, 2013; revision requested July 7 and received September 16; accepted September 19. For this journal-based SA-CME activity, the authors S.M. and K.A.F. have disclosed financial relationships (see p 699); the other authors, editor, and reviewers have no relevant relationships to disclose. **Address correspondence to** R.K.J.B. (e-mail: *rkjbrown@med.umich.edu*).

SA-CME LEARNING OBJECTIVES

After completing this journal-based SA-CME activity, participants will be able to:

■ Describe the process of neuronal uptake and cerebral biodistribution of FDG and identify normal cortical and subcortical structures at FDG PET.

■ Discuss the role of FDG PET in the diagnosis of primary neurodegenerative disorders and recognize the patterns of hypometabolism that typically characterize these disorders.

■ Discuss the emerging utilization of computer-assisted diagnosis in the evaluation of patients with dementia.

See www.rsna.org/education/search/RG.

TEACHING POINTS

See last page

The diagnosis of dementia syndromes can be challenging for clinicians, particularly in the early stages of disease. Patients with higher education levels may experience a marked decline in cognitive function before their dementia is detectable with routine testing methods. In addition, comorbid conditions (eg, depression) and the use of certain medications can confound the clinical assessment. Clinicians require a high degree of certainty before making a diagnosis of Alzheimer disease or some other neurodegenerative disorder, since the impact on patients and their families can be devastating. Moreover, accurate diagnosis is important because emerging therapeutic regimens vary depending on the cause of the dementia. Clinically based testing is useful; however, the results usually do not enable the clinician to make a definitive diagnosis. For this reason, imaging biomarkers are playing an increasingly important role in the workup of patients with suspected dementia. Positron emission tomography with 2-[fluorine-18]fluoro-2-deoxy-D-glucose allows detection of neurodegenerative disorders earlier than is otherwise possible. Accurate interpretation of these studies requires recognition of typical metabolic patterns caused by dementias and of artifacts introduced by image processing. Although visual interpretation is a vital component of image analysis, computer-assisted diagnostic software has been shown to increase diagnostic accuracy.

Introduction

Early diagnosis and characterization of dementia is a growing challenge in medicine. Primary neurodegenerative disorders are the leading cause of dementia and are characterized by progressive, accumulative damage to neuronal structures and interconnectivity, with clinical consequences of memory loss and progressive impairment of higher cognitive functions, leading to social and occupational dysfunction (1). In the United States, these disorders affect more than 14% of the population over 65 years of age and more than 50% of individuals older than 85 years (2–4). Alzheimer disease is the most common cause of dementia in the elderly and is the fourth leading cause of death in individuals over 65 years of age (1,2,4,5). Other frequently encountered disorders include frontotemporal dementia (FTD) and dementia with Lewy bodies (DLB). Alzheimer disease accounts for 50%–60% of dementias, with FTD

and DLB each accounting for approximately 15%–25% (5,6). It is important to accurately distinguish between these disorders because appropriate treatment depends on the specific diagnosis, and the use of expensive and possibly ineffective medications can be avoided. In addition, certain medications can have adverse effects on patients with DLB.

The diagnosis of a primary neurodegenerative disorder is commonly made by excluding secondary causes. The workup of patients with cognitive impairment involves anatomic imaging (computed tomography [CT] and magnetic resonance [MR] imaging) performed concurrently with biochemical and laboratory investigations to exclude dementia due to structural, vascular, metabolic, inflammatory, hormonal, or toxic causes. However, once these secondary causes have been ruled out, anatomic imaging techniques are limited in their ability to help distinguish between various forms of dementia, since atrophy and ventricular enlargement are often late signs of disease (7,8). Histopathologic analysis is the standard of reference for the diagnosis of Alzheimer disease. The presence of intraneuronal deposits of abnormally phosphorylated τ protein (neurofibrillary tangles) and extracellular β-amyloid (senile plaques) are seen in Alzheimer disease. However, brain biopsies are not practical for routine clinical workup. Distinguishing between different neurodegenerative disorders on the basis of clinical assessment alone may be difficult. Diagnosis is particularly challenging in the early stages of disease, especially in patients with higher levels of education who may experience significant decline in cognitive function before being recognized as having cognitive impairment on standardized neuropsychologic tests (9–11). Furthermore, comorbid conditions (eg, depression) and the use of certain medications can confound the clinical assessment.

Positron emission tomography (PET) with 2-[fluorine-18]fluoro-2-deoxy-D-glucose (FDG) is a highly useful imaging modality for the diagnosis of neurodegenerative disorders (1–6). FDG is an analog of glucose, the main energy substrate of the brain. After uptake and phosphorylation by hexokinase, FDG becomes trapped in neurons, allowing imaging and measurement of the cerebral metabolic rate for glucose. This is closely related to neuronal and synaptic function in numerous human resting and functional activation studies (1–3). Characteristic patterns of altered metabolism seen at FDG PET can markedly improve the clinical diagnosis for specific types of dementia such as FTD, Alzheimer disease, and DLB, each of which has characteristic metabolic signatures, although there is some overlap. An essentially normal or preserved cerebral uptake pattern can also help distinguish reversible pseudodementia due to depression from a primary neurodegenerative syndrome (12,13). Recognition of the common patterns of altered cortical metabolism seen in these various entities is crucial for identifying the cause of cognitive impairment. With use of proper technique, and with the increasing availability of computer-assisted diagnostic (CAD) statistical mapping tools, the neuroimager can play a key role in the workup of patients with cognitive impairment.

In this article, we discuss brain FDG PET in terms of patient preparation, image acquisition, and image processing and display. In addition, we review the characteristic metabolic patterns seen in various causes of dementia and discuss pitfalls, quality control issues, artifacts, and factors that may confound image interpretation.

Brain FDG PET

Patient Preparation

The patient should fast for at least 4 hours before the injection of a standard dose of 5–10 mCi (185–370 MBq) of FDG via a peripheral cannula. Serum glucose levels should be determined at the time of the injection and recorded in the final report, with a level under 140 mg/dL being desirable, although this cannot always be achieved in diabetic patients. Elevated glucose levels can interfere with FDG uptake in the brain (14). The patient should be well hydrated to encourage renal clearance of radioactivity and should be instructed to void prior to imaging to improve target-to-background counts and decrease unnecessary exposure of the bladder to radioactivity. If the patient is receiving fluids intravenously, the use of dextrose should be avoided. A relevant history should be recorded, including reason for examination, any prior surgery or trauma (eg, craniotomy, seizures, closed head injury), and medications (eg, benzodiazepines, barbiturates) that could alter the biodistribution of FDG in the central nervous system or peripherally. After injection, the patient remains in a quiet, darkened uptake room and is instructed to stay awake, keep his or her eyes open, and not vocalize, thereby ensuring standardization of cerebral uptake before imaging. The uptake of FDG when the patient's eyes are closed may cause hypometabolism in the occipital lobe, possibly leading to a misdiagnosis of DLB.

Image Acquisition

Brain FDG PET is typically performed 30 minutes after injection. Imaging is performed

with the PET camera in three-dimensional (3D) mode with septa removed for improved sensitivity and the PET camera detectors positioned over the patient's head perpendicular to the orbital-meatal line. Imaging usually takes about 15 minutes, although actual acquisition time varies depending on the scanner and the injected dose. Scatter correction– and time of flight–capable systems can generate satisfactory images with shorter acquisition times. It is important to instruct the patient to keep the head still during image acquisition, since movement of the head can interfere with image quality and compromise the validity of the attenuation correction algorithm. At our institution, brain PET is performed on a Siemens Biograph mCT scanner (Siemens Medical Solutions, Hoffman Estates, Ill). Nondiagnostic CT (30 mAs, 130 kV), is performed with the patient in the same bed position as for PET, and the resulting data are then used for attenuation correction as well as anatomic correlation.

Image Processing and Display

Following tomographic reconstruction with scatter correction and resolution recovery, CT-based attenuation correction is applied. Postprocessing consists of image reorientation, usually to a canthocaudal orientation, and normalization of uptake. Once processed, the images can be displayed in standard gray scale on a diagnostic monitor. Images obtained in all three projections (axial, coronal, and sagittal) should be reviewed. Use of color enhancement can aid in demonstrating subtle areas of altered metabolism. Several CAD software programs are available for brain image interpretation, all of which work on the same basic principle (15). These programs are designed to standardize brain images to account for individual variations in head size and shape and achieve correct alignment in the anterior commissure–posterior commissure plane, thereby allowing regional correlation with available brain atlases. The mapping of data to a brain FDG PET template then allows comparison of activity between individuals or groups of patients with use of statistical modeling, enabling the display of significant hypometabolic voxels on either two-dimensional cross-sectional images or 3D surface-rendered images and thereby facilitating pattern recognition, which is the key to the diagnosis (15). Use of automated voxel-based statistical mapping of the brain has been shown to increase diagnostic accuracy (16). The Z-score is the number of standard deviations from a database of age-matched control subjects and may be displayed with voxel-based color coding.

Reorientation, Reformatting, and Transformation.—PET data are mapped on a voxel-to-voxel basis to a standard brain template, which is designed to be compared with a brain atlas, the most commonly used of which is the Talairach atlas. This consists of a stereotactic atlas of digitized transaxial images with 50 standardized volumes of interest, including cortical (Brodmann) and subcortical regions. The process makes use of linear scaling to account for differences in individual brain size and nonlinear warping to minimize regional differences between findings in individuals and the atlas.

Normalization.—Activity in each voxel is normalized either globally or regionally (17). Regional normalization is performed to a selected region (eg, the cerebellum or pons) that is considered unlikely to be unaffected by the disease process (18).

Three-dimensional Stereotactic Surface Projection Display.—In addition to axial, sagittal, and coronal images, these programs allow surface-rendered displays. This method finds the highest activity voxel for a distance of 13 mm along a predefined vector angled perpendicular to the brain surface or medial outer cortex, and the maximum activity is assigned to the surface voxel (projected back). With this method, a large amount of information is condensed into a few hemispheric surface images on which the regional statistical deviation from the "normal" database can be overlaid.

MR Imaging Display.—Some programs allow PET data to be coregistered to a high-quality standard MR imaging template, allowing precise anatomic localization of regional cerebral hypometabolism.

Characteristic Metabolic Patterns of Neurodegenerative Disorders

Characterization of the major dementia syndromes requires knowledge of both the clinical and imaging data. Interpretation of the images alone can be misleading, since altered metabolism due to trauma, seizures, or vascular disorders can cause confusion. In addition, potential artifacts that can simulate disease may occur during image processing. However, before we discuss pathologic states and artifacts, it will be useful to discuss the normal biodistribution of FDG and the normal appearance of the neuroanatomy at brain PET.

In healthy subjects, the most intense FDG uptake occurs in the subcortical putamen, caudate nucleus, and thalamus, followed by high uptake in the cortical gray matter. The globus pallidus typically demonstrates mild uptake, and the white matter is relatively photopenic. Figure 1 shows

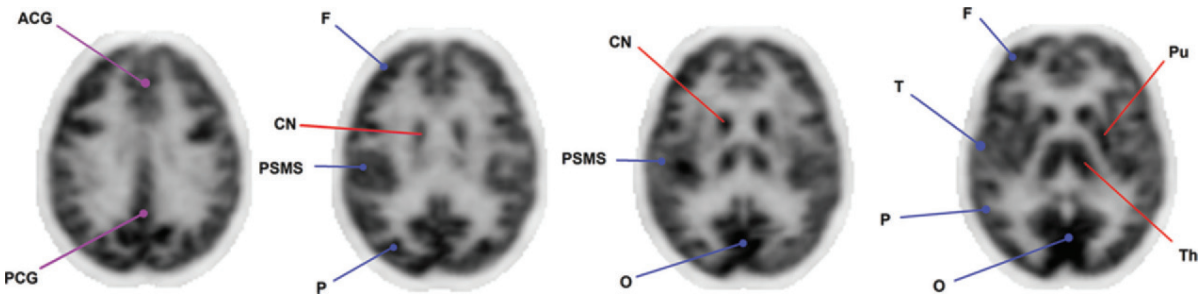

Figure 1. Sequential axial brain FDG PET images (transformed to a standardized, stereotaxic anatomic orientation [Talairach brain atlas space]) obtained in a normoglycemic patient starting approximately 30 minutes after injection show a stable pattern of cerebral uptake. The spatial resolution of PET allows identification of the cortical gray matter structures, white matter tracts, subcortical structures, and cerebellum. *ACG* = anterior cingulate gyrus, *CN* = caudate nucleus, *F* = frontal lobe, *O* = occipital lobe, *P* = parietal lobe, *PCG* = posterior cingulate gyrus, *PSMS* = primary sensorimotor strip, *Pu* = putamen, *T* = temporal lobe, *Th* = thalamus.

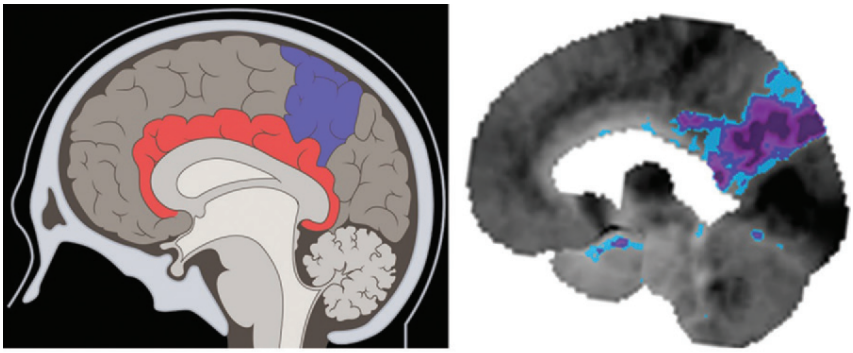

a. b.

Figure 2. Cingulate gyrus and precuneus. **(a)** Drawing (parasagittal view) shows the location of the cingulate gyrus (both anterior and posterior cingulate cortices) (orange) and the precuneus cortex (blue). The precuneus is bounded anteriorly by the marginal branch of the cingulate sulcus and posteriorly by the parieto-occipital sulcus. **(b)** Surface-rendered image shows FDG hypometabolism in the posterior cingulate and precuneus cortices. Blue = −2 SDs, purple = −3 SDs. The cingulate gyrus and precuneus are important structures to identify and analyze when reviewing brain FDG PET images obtained in patients with cognitive impairment.

neuroanatomic structures as seen at FDG PET. Two key structures to recognize are the cingulate gyrus and the overlying precuneus cortex, which are best appreciated on sagittal images of the medial hemispheres (Fig 2). The cingulate gyrus, located adjacent to the corpus callosum, is affected early in many neurodegenerative disorders. The precuneus lies cephalad to the posterior cingulate gyrus and is bounded anteriorly by the cingulate marginal sulcus and posteriorly by the parieto-occipital sulcus (Fig 2). Both structures should be actively sought and evaluated when analyzing images obtained for the workup of patients with dementia.

Alzheimer Disease

Alzheimer disease is the most common cause of dementia and is characterized by progressive cognitive decline, memory impairment, and an adverse impact on activities of daily living in middle-aged and elderly patients. At pathologic analysis, Alzheimer disease is characterized by early neuronal loss and gliosis in the mesiotemporal cortex and subsequent propagation to other brain regions. Pathologic hallmarks include β-amyloid plaques and neurofibrillary tangles formed from τ protein aggregates. The earliest changes of hypometabolism are often seen in the posterior cingulate gyrus (16). The classic pattern of impaired metabolism consists of involvement of the posterior cingulate gyri, precuneus, and posterior temporal and parietal lobes (19–24). With respect to the two hemispheres, involvement may be asymmetric or unilateral; when interhemispheric asymmetry is present, its direction is consistent across all involved regions (Fig 3). In addition, in nearly all cases, the posterior cingulate gyrus is preferentially involved (25,26). In more advanced Alzheimer disease, hypometabolism extends to involve the prefrontal

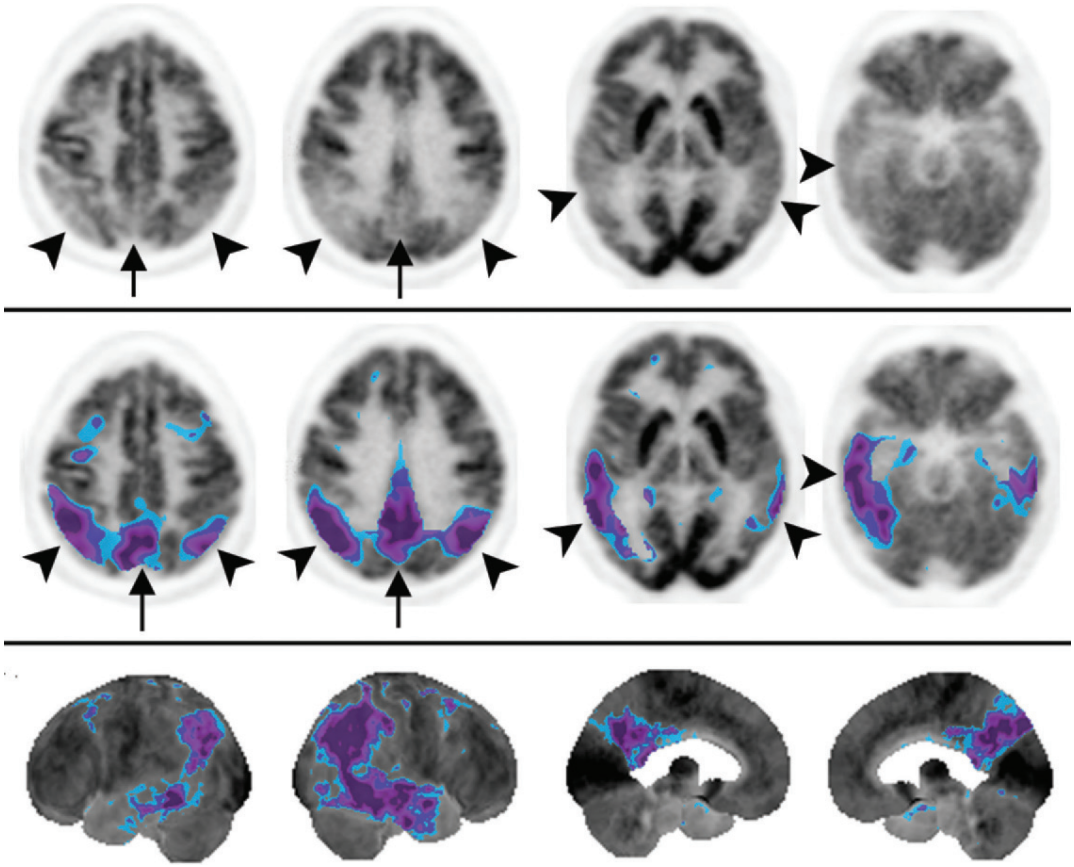

Figure 3. Alzheimer disease. Axial gray-scale FDG PET images (top), corresponding statistical thresholding overlay images (middle), and 3D stereotactic surface projection (SSP) images (bottom) (left to right: left lateral, right lateral, left medial, and right medial views) demonstrate bilateral hypometabolism in the parietotemporal cortices (arrowheads) and in the posterior cingulate–precuneus cortices (arrows), a pattern that is typical of Alzheimer disease. The posterior cingulate gyrus and precuneus are hypometabolic on the CAD images. Blue = −2 SDs, purple = −3 SDs. The earliest metabolic imaging biomarker of Alzheimer disease is often posterior cingulate gyrus hypometabolism. Although Alzheimer disease hypometabolism is frequently bilateral, defects are often asymmetric in extent and severity with respect to the left and right hemispheres; however, the posterior cingulate gyrus is usually involved. In more advanced Alzheimer disease, hypometabolism extends to involve the prefrontal association cortices as well. Metabolism is relatively preserved in the primary sensorimotor, visual, and anterior cingulate cortices, basal ganglia, thalamus, and posterior fossa structures in typical Alzheimer disease. In advanced disease, there may be frontal lobe involvement, but the anterior cingulate gyrus is spared.

association cortices as well, and there may be frontal lobe involvement, but the anterior cingulate gyrus is spared. A key feature of advanced neurodegenerative disorders (Alzheimer disease, DLB, and FTD) is sparing of the sensorimotor cortex, which appears more conspicuous when contrasted with the adjacent hypometabolism. In addition, metabolism is typically relatively preserved in the visual and anterior cingulate cortices, basal ganglia, thalamus, and posterior fossa in Alzheimer disease (Fig 4).

Dementia with Lewy Bodies

DLB is the second most common neurodegenerative disorder in patients over 65 years of age. The classic clinical triad includes *(a)* fluctuating levels of cognitive arousal, *(b)* visual hallucinations, and *(c)* spontaneous parkinsonism. In addition, the patient's clinical condition may worsen following the administration of neuroleptic medications (27–31). DLB manifests with a pattern of bilateral parietal and posterior temporal hypometabolism and posterior cingulate gyral hypometabolism similar to that seen in Alzheimer disease (32–34). However, there can also be associated involvement of the occipital lobes, which are spared in Alzheimer disease (35–37). This involvement of the occipital lobes is compatible with the clinical diagnosis of DLB (Fig 4). If the occipital cortex is not involved,

Teaching Point

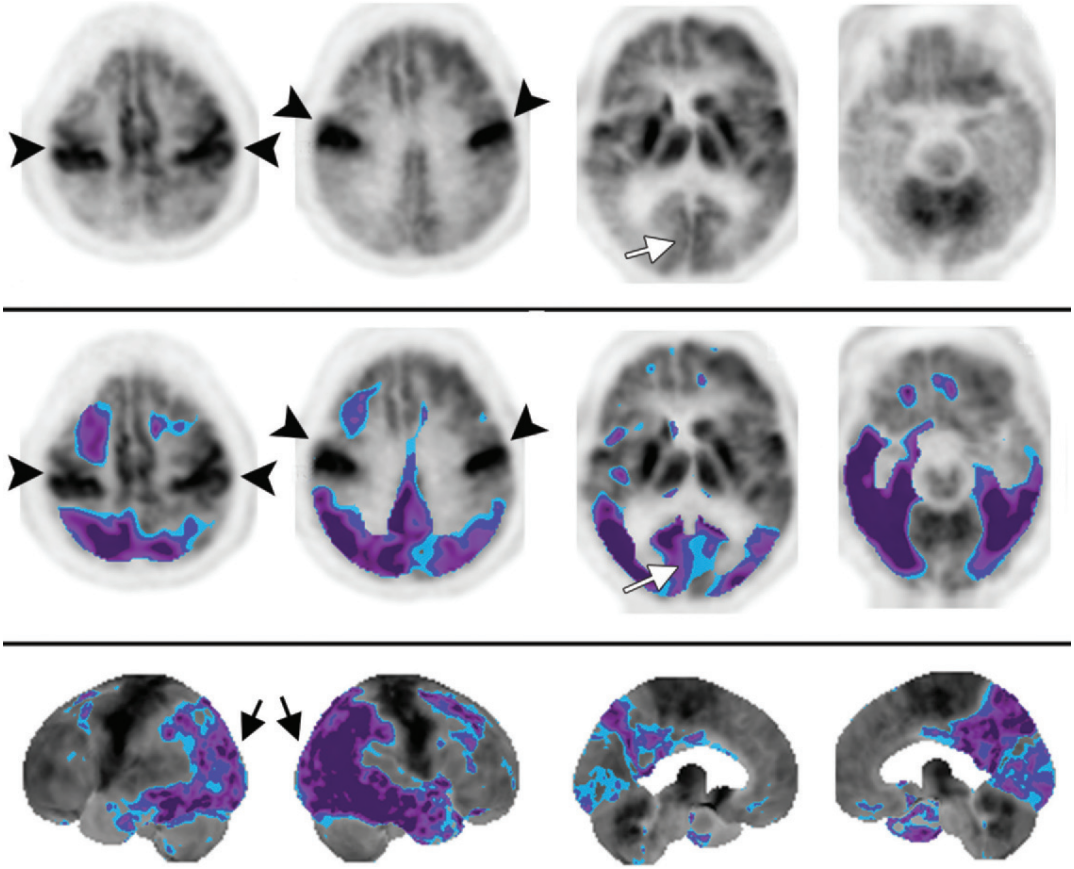

Figure 4. DLB. Axial gray-scale FDG PET images (top), corresponding statistical thresholding overlay images (middle), and 3D SSP images (bottom) (left to right: left lateral, right lateral, left medial, and right medial views) show severe bilateral prefrontal, parietal, temporal lobe, and posterior cingulate–precuneus cortical hypometabolism, findings that are typical of Alzheimer disease. However, there is additional hypometabolism in the occipital lobes, including the primary visual cortex (arrows), a finding that is diagnostic for DLB. Primary visual cortical hypometabolism is highly specific and moderately sensitive for distinguishing DLB from Alzheimer disease. In this case, preserved metabolism in the primary sensorimotor strip is relatively conspicuous (arrowheads) due to hypometabolism in both adjacent frontal and parietal association cortices. Note also the greater extent and intensity of hypometabolism throughout the involved regions of the right posterior parietotemporal cortices, a finding that can be seen in both DLB and Alzheimer disease. Blue = −2 SDs, purple = −3 SDs.

Alzheimer disease and DLB cannot be distinguished on the basis of their FDG metabolic signatures. Imaging with dopamine transporter agents can also help distinguish DLB from Alzheimer disease when clinical and FDG imaging findings are indeterminate (32,38). An Alzheimer disease pattern of hypometabolism and a positive dopamine transporter scan indicate that DLB is the most likely diagnosis. Findings of DLB include loss of dopaminergic neurons in the substantia nigra and related reduced striatal dopaminergic activity; therefore, patients with DLB have abnormal striatal uptake on dopamine transporter scans. Abnormal findings at dopamine transporter scanning performed with iodine 123 ioflupane are compatible with Parkinson disease or related neurodegenerative disorders such as parkinsonian dementia or DLB.

Frontotemporal Dementia

FTD is a neurodegenerative disorder with a predilection for the frontal and temporal lobes (Fig 5). Unlike for Alzheimer disease, there are no approved pharmacologic interventions for FTD, and the use of anticholinesterase-type medications should be avoided. Patients often present with social impairment and disinhibitive and impulsive behavior (39,40). FTD is the archetypal disorder in the group collectively known as frontotemporal lobar disorders, which include temporal variant FTD, or semantic dementia, and a frontal-predominant variant; these disorders have different clinical manifestations and distinct metabolic markers (Fig 6) (41–47).

Classic FTD is characterized by hypometabolism in the frontal and anterior temporal lobes with involvement of the anterior cingulate gyrus

Teaching Point

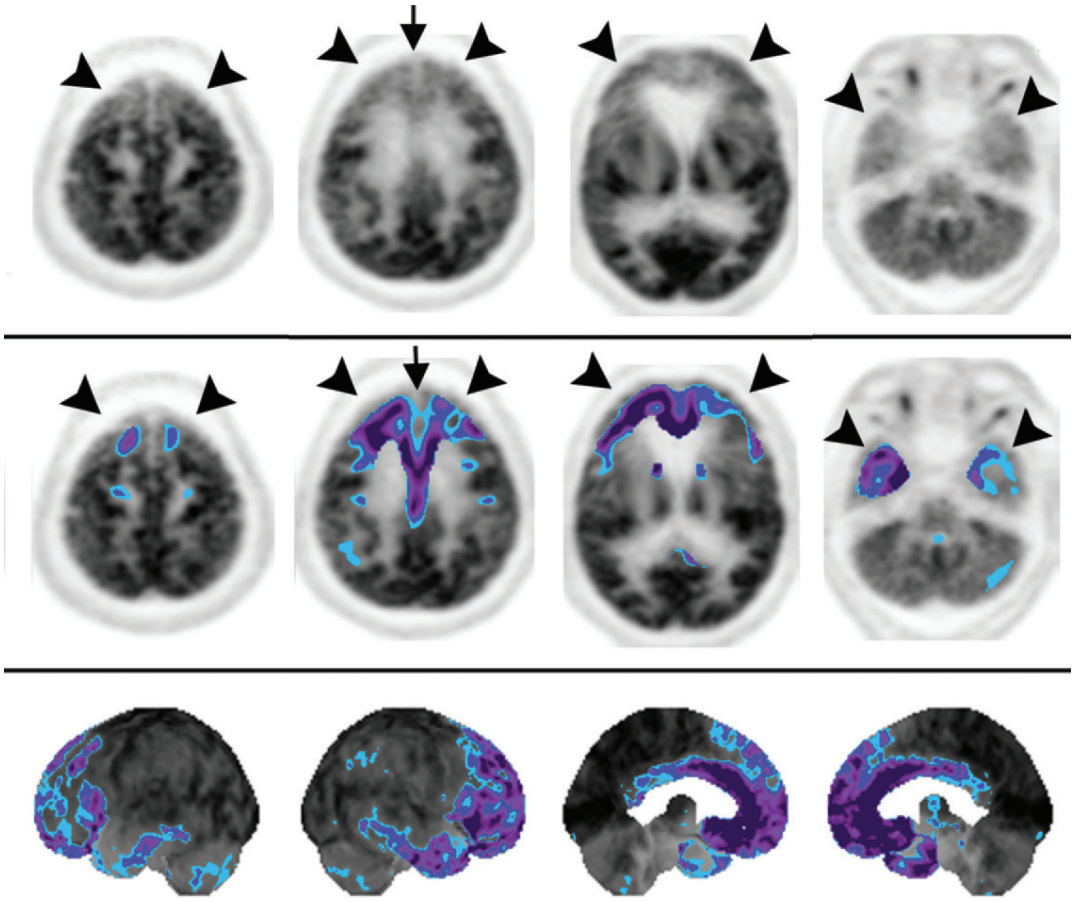

Figure 5. FTD. Axial gray-scale FDG PET images (top), corresponding statistical thresholding overlay images (middle), and 3D SSP images (bottom) (left to right: left lateral, right lateral, left medial, and right medial views) show moderate bilateral frontal and anterior temporal lobe hypometabolism (arrowheads) in a pattern that is characteristic of behavioral variant FTD. There is anterior cingulate gyral hypometabolism (arrows) as well as relatively preserved posterior cingulate–precuneus metabolism, findings that are best appreciated on the 3D SSP images. Blue = −2 SDs, purple = −3 SDs.

(41–47). Unlike in Alzheimer disease, involvement of the temporal lobes in FTD extends to their anterior aspects. The frontal-predominant form of FTD shows sparing of the temporal lobes, with patients typically demonstrating behavioral changes, including disinhibition. Patients with temporal variant FTD (semantic dementia) have problems with language and often cannot find the words to describe an object. For example, if they were given a hammer, they would know how to use it, but they may not be able to tell you that it is a hammer. These patients tend to have primarily temporal lobe hypometabolism (41).

Rare Neurodegenerative Disorders

Corticobasal degeneration is a rare neurodegenerative disorder that may manifest with asymmetric dystonia, and patients may present with "alien limb syndrome" (5,6). The key imaging features are a striking asymmetric involvement of the sensorimotor cortex and hypometabolism in the ipsilateral basal ganglia or thalamus. There is also involvement of the midportion of the cingulate gyrus and asymmetric atrophy of the frontal and parietal cortices (Fig 7).

Posterior cerebral atrophy (PCA) is another rare disorder that commonly manifests with complex visual cognitive changes. PCA is an atypical

Figure 7. Corticobasal degeneration. Axial gray-scale FDG PET images (top), corresponding statistical thresholding overlay images (middle), and 3D SSP images (bottom) (left to right: left lateral, right lateral, left medial, and right medial views) show the key features of corticobasal degeneration: hypometabolism in the primary sensorimotor cortex (arrowheads) and hypometabolism in the ipsilateral basal ganglia and the left thalamus (arrows). Asymmetric atrophy of the frontal and parietal cortical regions of the brain is also seen. Blue = −2 SDs, purple = −3 SDs. Many patients with corticobasal degeneration present with alien limb syndrome. ▶

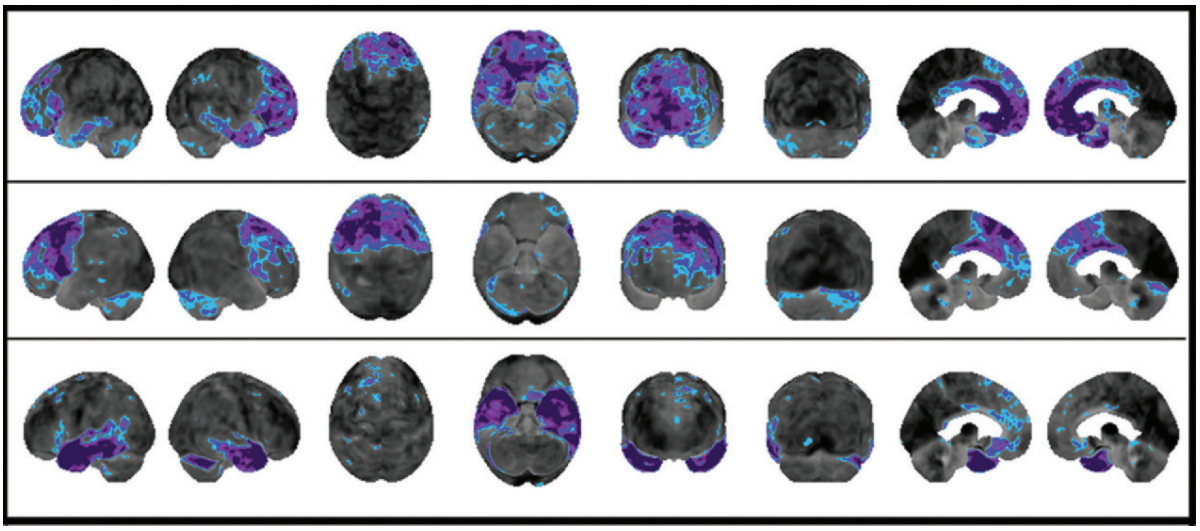

Figure 6. FTD variants. Three-dimensional SSP maps with overlaid Z-score statistical thresholds obtained in (left to right) the left lateral, right lateral, superior, inferior, anterior, posterior, left medial, and right medial projections. Z-score: blue = −2 SDs, purple = −3 SDs. There are three classic patterns seen in FTD, which have different clinical manifestations and distinct metabolic markers. Images in top row demonstrate how classic FTD is characterized by hypometabolism in the frontal and anterior temporal lobes with involvement of the anterior cingulate gyrus. These patients present with a history of disinhibited behavior and impaired language. Images in middle row demonstrate how, unlike in Alzheimer disease, involvement of the temporal lobes in FTD extends to their anterior aspects. Images in bottom row demonstrate the frontal-predominant form of FTD with sparing of the temporal lobes. These patients typically demonstrate disinhibited behavior and may have an atypical parkinsonian syndrome known as progressive supranuclear palsy. At FDG PET, semantic dementia manifests as prominent asymmetric or symmetric temporal hypometabolism.

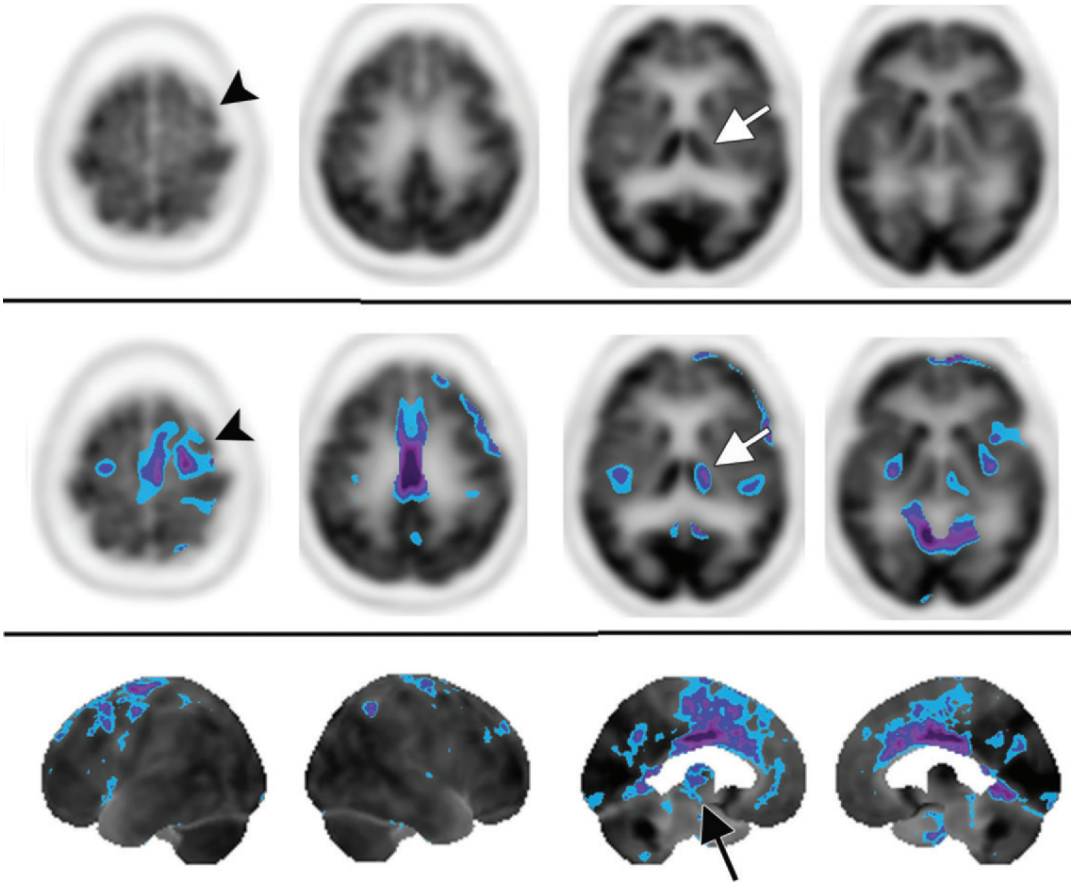

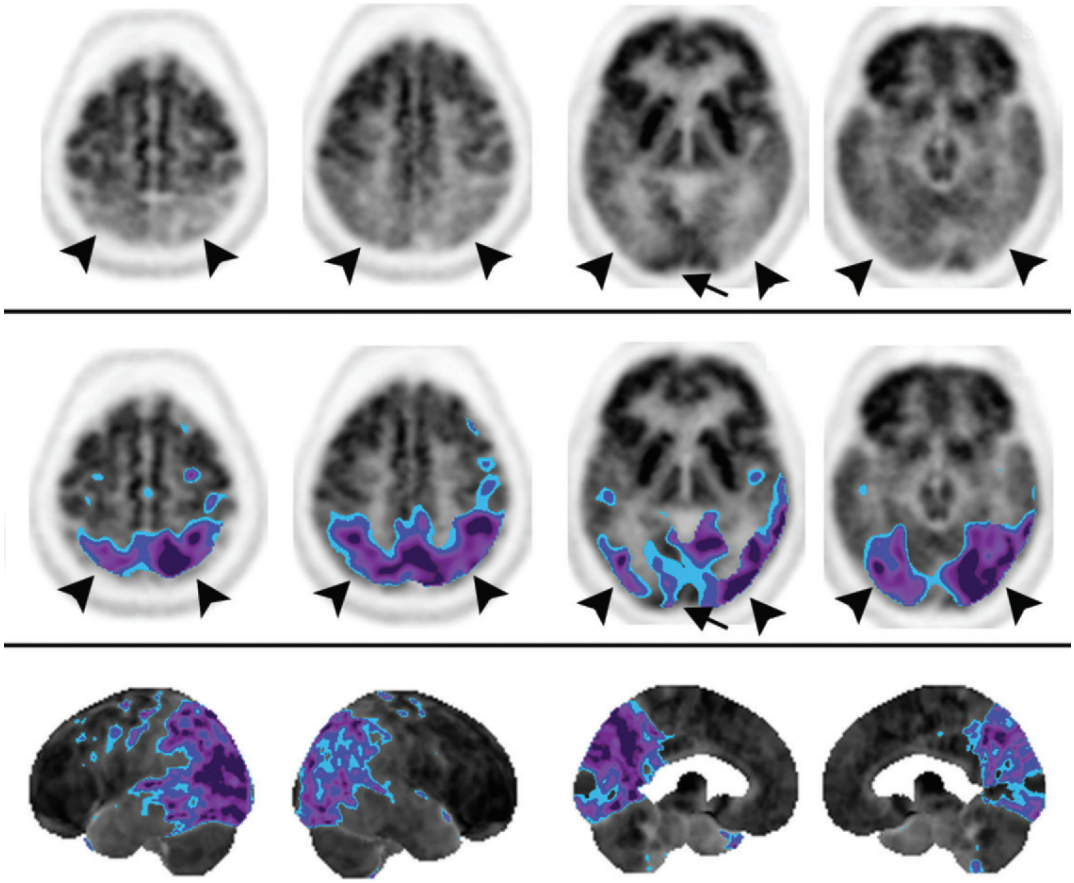

Figure 8. PCA. Axial gray-scale FDG PET images (top), corresponding statistical thresholding overlay images (middle), and 3D SSP images (bottom) (left to right: left lateral, right lateral, left medial, and right medial views) show posterior parietotemporal and occipital hypometabolism (arrowheads). An atypical variant of Alzheimer disease, PCA is characterized by a posterior cortical hypometabolic pattern of Alzheimer disease but with additional involvement of the lateral occipital association cortices (arrows). Blue = −2 SDs, purple = −3 SDs. Patients with PCA show a progressive, dramatic, and relatively selective decline in visual association skills.

variant of Alzheimer disease; however, whereas Alzheimer disease is most commonly associated with deterioration in memory and language, PCA patients show a progressive, dramatic, and relatively selective decline in visual association skills (Fig 8) (5,6).

Patterns of altered metabolism seen with 3D SSP statistical mapping are summarized in Figure 9. The Table summarizes the brain FDG PET patterns of hypometabolism seen in various neurodegenerative disorders.

Vascular Dementia and Other Conditions

Strokes are a common occurrence that are usually clinically apparent, are associated with clear changes at CT or MR imaging, and rarely manifest as an unexplained dementia syndrome. In our clinical practice, PET of vascular dementia is rare, likely due to a declining prevalence of multi-infarct dementia with improved treatment of hypertension and hyperlipidemia. In addition, patients with evidence of prior extensive vascular injury at CT or MR imaging are unlikely to be referred for an expensive study such as PET to make the diagnosis (48–51). Hypometabolism related to stroke is more likely to be encountered incidentally in patients undergoing routine PET for oncologic indications when at least a portion of the involved area is within the field of view. The typical pattern consists of hypometabolism with abrupt margins in the territory of either the anterior, middle, or posterior cranial arteries, usually with evidence of encephalomalacia in the corresponding region on the CT images (50–52). If the frontal lobe or internal capsule is involved, hypometabolism in the contralateral cerebellum may be seen due to crossed cerebrocerebellar diaschisis (Fig 10). Although multi-infarct dementia can be caused by both large and small vessel disease, vascular dementia is now manifesting more commonly with subcortical ischemic disease due to the presence of small rather than large vessel disease (53–58).

Brain FDG PET Patterns of Hypometabolism in Neurodegenerative Disorders

Brain Region	Disorder				
	Alzheimer Disease	DLB	PCA	FTD	Corticobasal Degeneration
Bilateral posterior parietotemporal	↓	↓	↓	Initially preserved, later ↓	Preserved to asymmetric reduction
Posterior cingulate	↓	↓	↓	Initially preserved, later ↓	Asymmetric ↓
Anterior cingulate	Preserved	Variable	Preserved	↓	↓
Frontal lobe	Mild ↓ (more with advanced disease)	↓ (more with advanced disease)	Preserved	↓	Asymmetric ↓
Anterior temporal lobe	Relatively preserved	Variable	Preserved	↓	Preserved
Basal ganglia	Preserved	↓ (caudate)	Preserved	Variable to preserved	Asymmetric ↓
Primary sensorimotor cortex	Preserved	Preserved	Preserved	Variable to preserved	Asymmetric ↓
Primary and associative visual cortex	Preserved	↓ in medial occipital cortex (primary visual)	↓ in lateral occipital cortex (visual association)	Preserved	Preserved

Note.—↓ = hypometabolism.

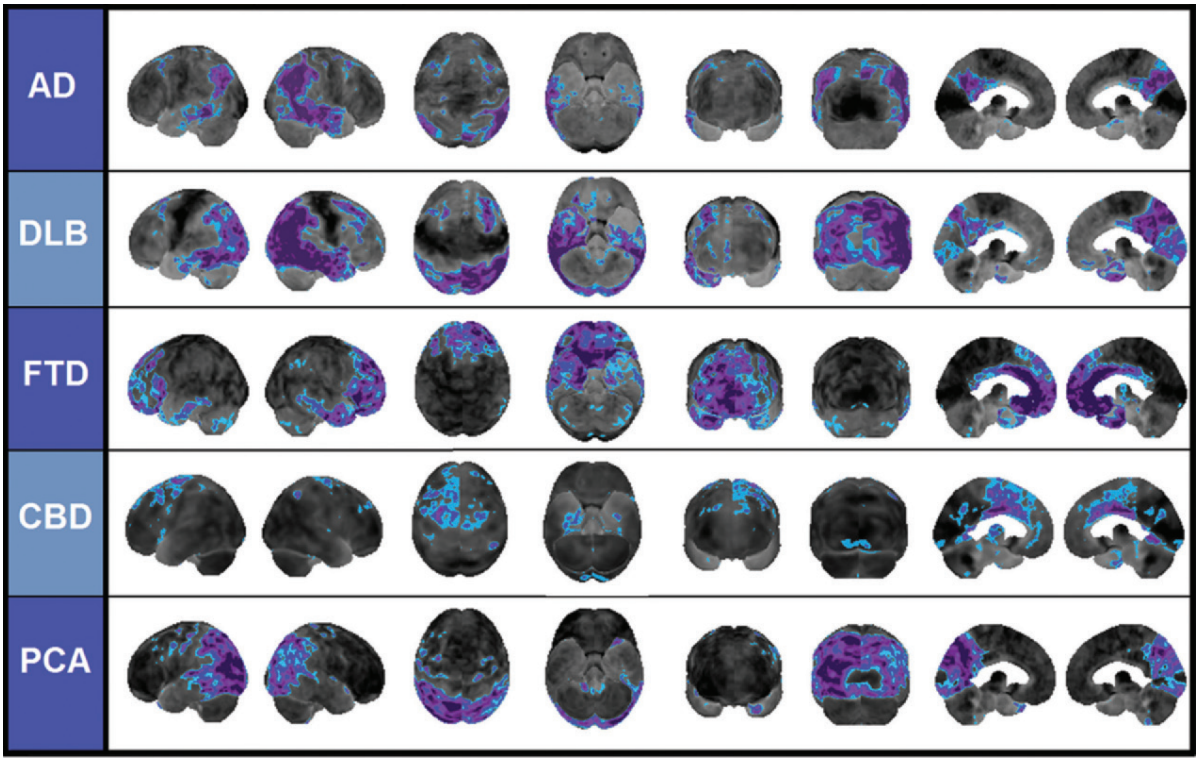

Figure 9. Rows of 3D SSP maps with overlaid Z-score statistical thresholds demonstrate composite patterns of cerebrocortical hypometabolism in various causes of dementia. *AD* = Alzheimer disease, *CBD* = corticobasal degeneration. Images were obtained in (left to right) the left lateral, right lateral, superior, inferior, anterior, posterior, left medial, and right medial projections. Z-score: blue = −2 SDs, purple = −3 SDs.

Figure 10. Crossed cerebrocerebellar diaschisis. Axial PET images obtained at the level of the basal ganglia (left) and cerebellum (middle) and posterior maximum intensity projection image (right) demonstrate right-sided vascular brain disease, with decreased metabolism seen in the contralateral cerebellar hemisphere (arrowheads). The atrophic effects of crossed cerebrocerebellar diaschisis may take years to manifest at anatomic imaging. However, altered metabolism appears much earlier.

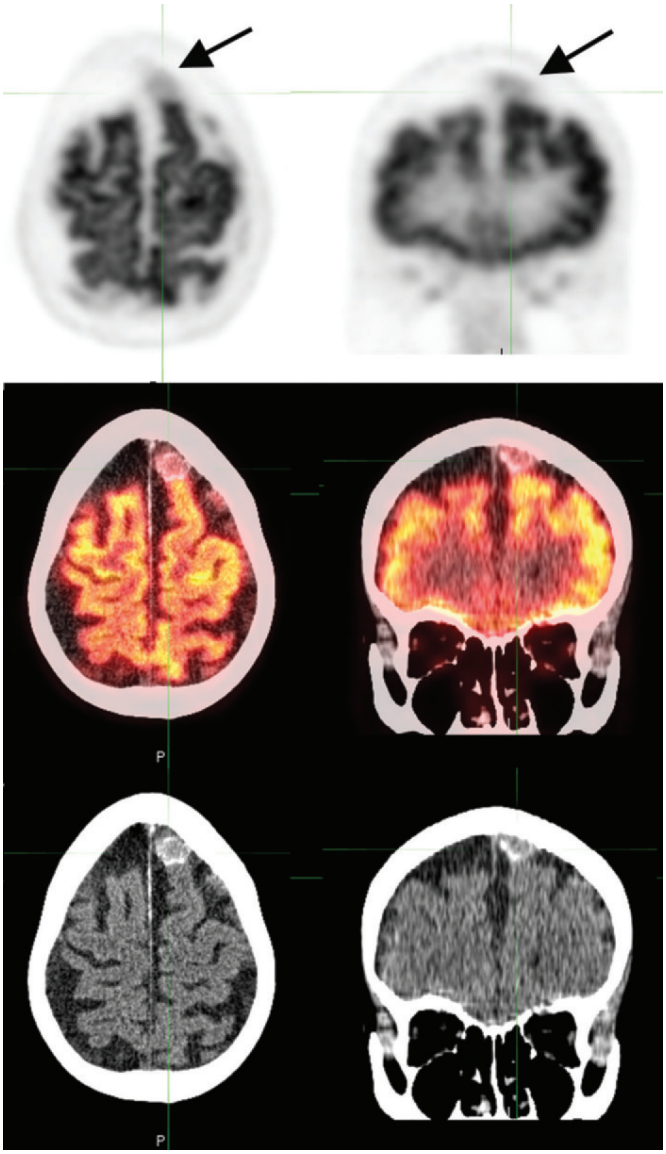

Figure 11. Meningioma. Axial (top left) and coronal (top right) gray-scale FDG PET images, axial (middle left) and coronal (middle right) fused PET/CT images, and axial (bottom left) and coronal (bottom right) CT images show a meningioma with mild uptake (arrows). Many intracranial lesions may appear to be hypometabolic relative to the gray matter cortex, and correlation with MR imaging and CT findings is crucial to avoid missing these lesions.

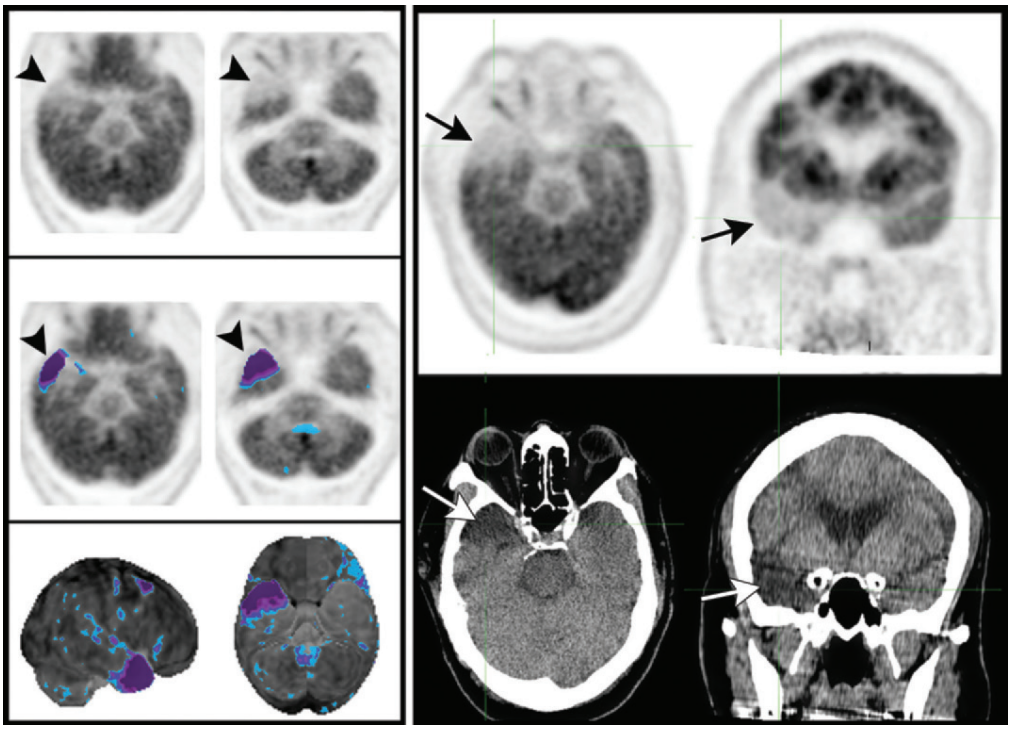

Figure 12. Arachnoid cyst. Axial gray-scale FDG PET images (top left), corresponding statistical thresholding overlay images (middle left), and 3D SSP images (bottom left) obtained in the right lateral (left) and inferior (right) projections demonstrate hypometabolism in the anterior aspect of the right temporal lobe (arrowheads). This finding may be misinterpreted as the semantic or temporal variant of FTD if the CT images are not reviewed. In this case, however, the finding is caused by an arachnoid cyst, not a neurodegenerative condition, as indicated by an arrow on axial and coronal PET images (top right) and axial and coronal coregistered CT images (bottom right). Z-score: blue = −2 SDs, purple = −3 SDs.

Pitfalls, Quality Control Issues, and Artifacts

It is important to review the anatomic (ie, CT or MR) images before interpreting the PET study. Structural lesions such as tumors (Fig 11), extraaxial collections, encephalomalacia, and other lesions (Fig 12) may confound the interpretation. Proper inspection of the anatomic images will prevent false-positive errors. In the absence of anatomic structural changes, the risk of false-positive findings at FDG PET for dementia is low, but such findings may be seen in rare pathologic conditions such as autoimmune encephalitis (59). Atrophy occurs with neurodegenerative disorders, although it may also be observed as part of the normal aging process (7,8). Reduction in brain volume may simulate hypometabolism, leading to artifacts at statistical parametric mapping (SPM) (Fig 13). Although the SPM software can be useful, it has limitations. In some patients, SPM may indicate that there is hypometabolism adjacent to the gray matter at the gray matter–white matter interface. This is an artifact due to a misregistration error in mapping and should not be confused with disease. The key to recognizing this artifact is knowing that it coregisters to the white matter and does not extend to the peripheral cortical margins (Fig 14). Patient motion can markedly alter the appearance of the attenuation-corrected images by creating regions of decreased activity due to an oversubtraction artifact, and this motion may not be apparent from viewing the PET images alone (Fig 15). A region of decreased metabolism that is seen only on the attenuation-corrected images is due to an attenuation correction artifact related to motion between the CT (anatomic) and PET (metabolic) images. This can be confirmed by viewing the CT and PET images in fused mode.

Discussion

The interpreting radiologist also needs to be aware of the terminology used by our neurology colleagues when reporting brain images. There is a spectrum of diminished function that ranges from mild cognitive impairment (MCI) to dementia. MCI is often regarded as an intermediate state between normal cognition and fully developed dementia. It can be defined on the basis of

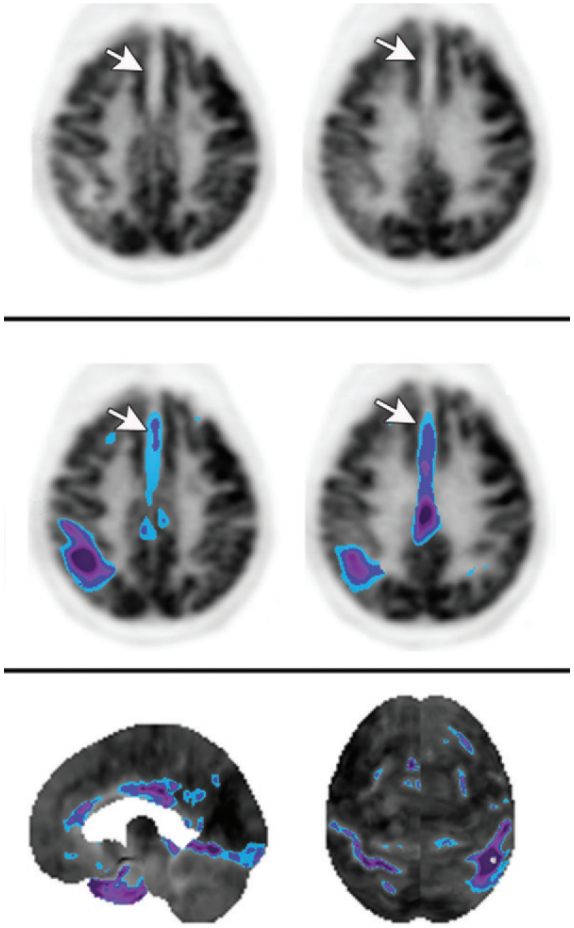

Figure 13. PCA. Axial gray-scale FDG PET images (top), corresponding statistical thresholding overlay images (middle), and 3D SSP images (bottom) obtained in the right medial (left) and superior (right) projections illustrate how interpretation should include review of both the Z-map images and the gray-scale data. The seemingly hypometabolic areas on the SPM images (arrows) are actually areas of atrophy localizing to and representing widening of the sulci and represent artifact rather than true hypometabolism in cortical gray matter. If not recognized, this potential pitfall can be confused with a neurodegenerative disorder, underscoring the need for careful review of the FDG images in native (patient) spatial orientation and of the reoriented (atlas space) images prior to the assessment of statistical maps. Blue = −2 SDs, purple = −3 SDs.

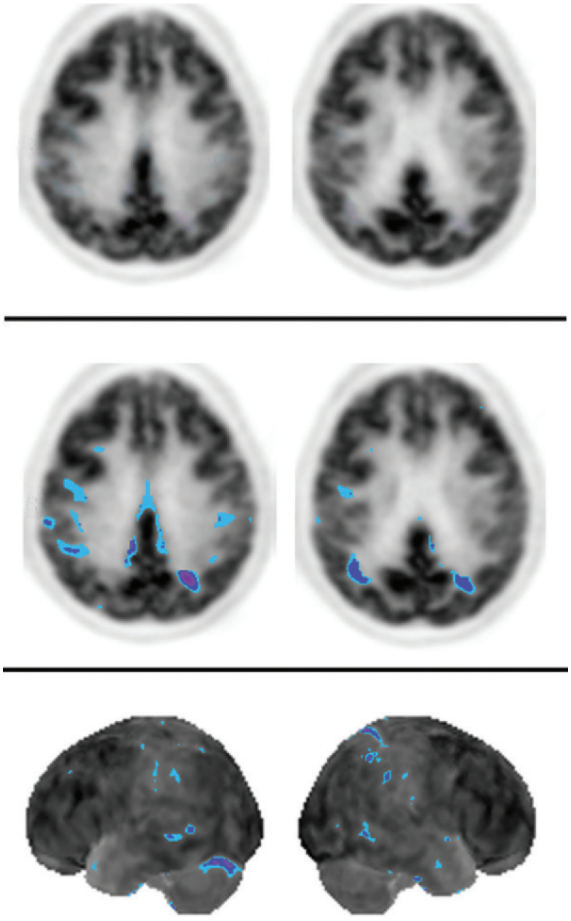

Figure 14. Effects of resolution and contrast disparity between individual scanning data and the normal database. Axial gray-scale FDG PET images (top), corresponding statistical thresholding overlay images (middle), and 3D SSP images (bottom) obtained in the left lateral (left) and right lateral (right) projections demonstrate apparent voxels with significant hypometabolism. As in Figure 13, the areas indicated as hypometabolic on the "computer-assisted" images are in fact areas of atrophy. However, the changes in the right posterior parietal region actually reflect a combination of atrophy and gyral hypometabolism. Blue = −2 SDs, purple = −3 SDs.

mildly reduced scores on simple cognitive screening tests, such as the Mini-Mental State Examination (MMSE) or Montreal Cognitive Assessment (MOCA), or defined more precisely on the basis of deficits in at least one cognitive domain at detailed neuropsychologic testing. Fully developed dementia is characterized by deficits that are not only more severe and extensive, affecting two or more cognitive domains, but are also of sufficient severity to affect the patient's activities of daily living. Therefore, clinical criteria (such as those created by the National Institute for Neurologic and Communicative Disorders and Related Disorders Association) combined with imaging and laboratory biomarkers are used for diagnosis (60,61). FDG PET for the evaluation of cognitive impairment has been found to help detect the earliest changes in neurodegenerative disorders and to help predict conversion from MCI to early Alzheimer disease. A small study in which SPM was used to compare 14 Alzheimer disease patients with 16 MCI patients found that the former group had reduced cerebral glucose metabolism in the posterior cingulate cortex, precuneus, and inferior parietal and middle temporal lobes, whereas in MCI patients, hypometabolism occurred only in the posterior cingulate gyrus

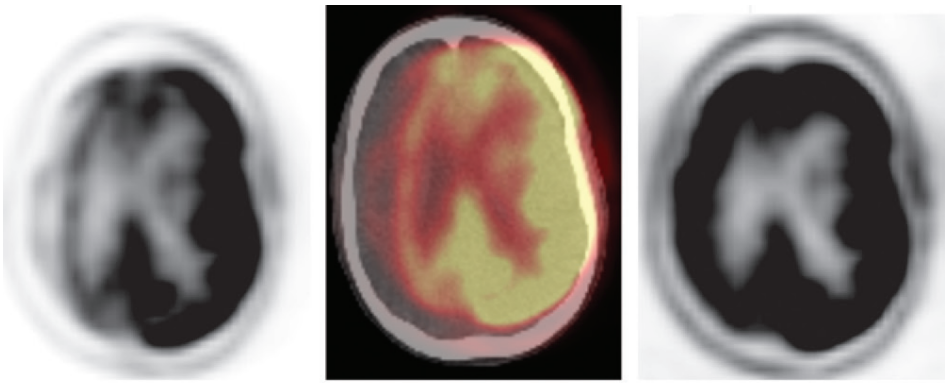

a. b. c.

Figure 15. Attenuation correction artifact due to misregistration. **(a)** Non–attenuation-corrected image shows no region of decreased activity. **(b)** On a fused PET/CT image, the datasets are not properly coregistered. This "misalignment" between the anatomic and metabolic images causes an artifact with apparent diminished activity. **(c)** Attenuation-corrected image shows a region of decreased activity, a finding that is artifactual and due to patient motion. Viewing the non–attenuation-corrected and fused PET/CT images is an important quality control check, since patient motion can introduce attenuation correction artifacts.

(20). It should be noted that MCI is a heterogeneous entity, but prospective studies have shown that patients with amnesic MCI that later converts to Alzheimer disease may already show an Alzheimer disease–like pattern of glucose hypometabolism at an early stage (62).

FDG PET is useful in differentiating between various types of primary dementia. In one multicenter study, 548 elderly subjects—including 110 healthy subjects—underwent FDG PET. Disease-specific patterns allowed correct classification in 95% of patients with Alzheimer disease, 92% of patients with DLB, 94% of patients with FTD, and 94% of healthy subjects (63). Of the patients with MCI, 81% were found to have posterior cingulate cortical and hippocampal (temporal) hypometabolism (63). A meta-analysis of 24 studies involving 1112 patients confirmed the ability of FDG PET to help predict the conversion of MCI to Alzheimer disease (64). FDG PET can depict glucose metabolic changes that not only precede but also exceed the degree of atrophy as determined with volumetric MR imaging, including voxel-based morphometry (65,66).

Because of coupling between glucose metabolism and regional cerebral perfusion, both FDG PET and regional cerebral blood flow single photon emission computed tomography (SPECT) performed with radiotracers such as technetium 99m (^{99m}Tc) hexamethylpropylenamine oxime (Ceretec; GE Healthcare, Little Chalfont, England) and ^{99m}Tc–ethyl cysteinate dimer (Neurolite; Lantheus Medical Imaging, North Billerica, Mass) can help identify the topographic patterns of the various dementias (67). However, comparative studies have shown FDG PET to be superior to regional cerebral blood flow SPECT (68). This is likely due to the higher intrinsic spatial resolution of PET and the improved attenuation correction algorithms used with 3D tomographic reconstruction. Other positron-emitting radiopharmaceutic agents are available that directly depict neural inflammation and neurotransmitter receptors, and recently, the U.S. Food and Drug Administration approved an amyloid contrast agent (florbetapir [Amyvid; Eli Lilly, Indianapolis, Ind]) for clinical use. Since October 2013, flutemetamol (Vizamyl, GE Healthcare) has also been approved.

Automated voxel-based statistical analysis has been uniformly used in FDG PET–based research to provide standardized, objective, and quantitative validation of observed metabolic changes in neurodegenerative disorders (15). Several studies have examined the accuracy of automated systems versus expert readers to determine their diagnostic performance as an automated, hands-off process, and to evaluate how their use may affect or improve clinical diagnostic interpretation (69,70). Studies have found that the performance of automated systems and expert readers is equivalent with respect to receiver operating curve characteristics for all types of neurodegenerative disorders. The use of automated readers has also been shown to improve the learning curve of beginning readers. This is to be expected, since brain imaging, unlike oncologic imaging, does not require visualization of increased "hot spot" uptake for diagnosis. It is difficult to detect small changes of reduced activity, including localization, with the human eye, against a background of high cerebral glucose biodistribution with variations in normal from

patient to patient. In addition, although a group of patients with one type of neurodegenerative disorder may all have the same basic imaging findings, each individual patient may have his or her own pattern with variations in symmetry, severity, and areas affected. Some brain regions such as the posterior cingulate gyrus and precuneus are not well appreciated on axial images, so that subtle metabolic changes may be difficult to detect without a CAD tool. In the late stages of neurodegenerative disorders, altered metabolism becomes more widespread, and several disorders may converge, partly due to the complex interconnectivity of the neuronal regions. FDG PET findings at automated software analysis have also been correlated with different clinical patterns of presentation (71). In a study by Patterson et al (26), objective analysis of FDG PET images using SPM improved the detection of subtle abnormalities compared with subjective criteria alone. The authors found that, in the evaluation of early- and late-onset Alzheimer disease, the diagnostic performance of a fully automated system using SPM was similar to that of expert readers and slightly superior to that of beginning readers (26). This suggested that use of automatic readers could improve the learning curve of beginners (25). Automated voxel-based statistical analysis as an adjunct clinical tool therefore has great potential for improving accuracy, reducing interobserver variation, and training novice readers.

It is increasingly being recognized that a patient who is being referred for a diagnostic imaging study for dementia may have a mixture of causal pathologic processes (72,73). The presence of a comorbid condition (eg, cerebrovascular disease or mixed Alzheimer disease and DLB) may confound the interpretation of the imaging study. Therefore, complex brain FDG PET findings that cannot be readily classified as Alzheimer disease, DLB, or FTD should be considered as indicating the presence of multiple pathologic conditions. In this respect, review of anatomic neuroimaging studies (eg, MR imaging) is critical in evaluating for comorbid cerebrovascular disease or prior head injury for more accurate assessment of brain FDG PET studies. Apart from mixed or overlapping pathologic conditions, dementia syndromes may also have atypical manifestations. In particular, Alzheimer disease has been found to sometimes manifest with so-called focal cortical findings, which may be classified with FDG PET as FTD, corticobasal degeneration, or PCA (74). These findings indicate that Alzheimer disease is a much more common cause of focal cortical syndromes than was previously recognized (74). Alzheimer disease can also manifest as a frontal variant, with more prominent early findings of frontal hypometabolism in addition to the typical posterior cortical hypometabolic changes.

Atypical FDG PET findings in dementia patients can be further evaluated with the use of disease-specific imaging or fluid biomarkers for a more precise assessment of causal pathologic processes (75). For example, the combined use of β-amyloid (eg, PET with florbetapir) and dopamine transporter or nerve terminal imaging (eg, SPECT with ioflupane dopamine transporter imaging) is now being studied as a diagnostic stratification approach for the refinement of workup for dementia (76). With this schema, typical FTD would manifest with negative amyloid and grossly normal dopamine transporter scans, and striatal dopamine transporter scans would be abnormal in DLB but normal in Alzheimer disease, Amyloid scans would be positive in typical Alzheimer disease, whereas DLB can manifest with positive amyloid scans in over one-half of patients. Note that application of this proposed schema remains investigational, and that further studies are needed to determine the possibility of false-positive classifications.

Some drugs are also well known to induce cerebral glucose metabolic changes. For example, the use of diazepam for sedation has been found to reduce cerebral glucose metabolism globally by about 20% (72). A study by Wang et al (73) found that lorazepam significantly decreased whole-brain metabolism by over 10%. Although regional cerebral effects may affect subcortical structures such as the thalamus, cortical effects generally tend to be more diffuse and are not expected to significantly affect the specific topographic cortical patterns of the major dementia syndromes. Nevertheless, it is recommended that benzodiazepine be administered for sedation after the 30-minute FDG uptake phase prior to imaging.

Although there is presently no clinical indication for repeat FDG PET to monitor disease progression or treatment response in dementia patients, equivocal and nondiagnostic findings at early imaging may warrant repeat FDG PET in 6–12 months in cases in which the patient demonstrates progressive cognitive decline. There are no consistent reported glucose metabolic changes associated with currently approved treatments for Alzheimer disease (cholinesterase inhibitors, memantine). Hence, there is no current practice standard for the imaging evaluation of treatment response. However, this may change in the future as new therapies become available.

Conclusion

FDG PET is a highly useful imaging modality for the diagnosis of primary neurodegenerative disorders. Patterns of altered cerebral glucose metabolism seen at FDG PET are useful as imaging

biomarkers to assist in making the clinical diagnosis of neurodegenerative diseases causing dementia. CAD software tools improve the learning curve and increase the accuracy of interpretation for these studies.

Acknowledgments.—The authors wish to acknowledge Mark Schechter, MD, for contributing a case to this manuscript, and Leslie Burrell for her contribution of a medical illustration.

Disclosures of Conflicts of Interest.—**K.A.F.:** *Related financial activities:* consultant for MIM Software. *Other financial activities:* consultant for Avid Pharmaceuticals, Bayer Schering Pharma, and GE Healthcare; grant from GE Healthcare; speakers bureau for the Society of Nuclear Medicine and Molecular Imaging, Johns Hopkins University, and Washington University in St Louis; honorarium from Eli Lilly; stockholder in GE, Novo Nordisk, Bristol-Myers Squibb, and Merck Pharmaceuticals. **S.M.:** *Related financial activities:* none. *Other financial activities:* consultant for Hamamatsu Photonics; grants from Philips Healthcare and Hitachi; royalties from GE Healthcare.

References

1. Gallucci M, Limbucci N, Catalucci A, Caulo M. Neurodegenerative diseases. Radiol Clin North Am 2008;46(4):799–817, vii.
2. Coleman RE. Positron emission tomography diagnosis of Alzheimer's disease. Neuroimaging Clin N Am 2005;15(4):837–846, x.
3. Silverman DH, Alavi A. PET imaging in the assessment of normal and impaired cognitive function. Radiol Clin North Am 2005;43(1):67–77, x.
4. Van Heertum RL, Tikofsky RS. Positron emission tomography and single-photon emission computed tomography brain imaging in the evaluation of dementia. Semin Nucl Med 2003;33(1):77–85.
5. Herholz K, Carter SF, Jones M. Positron emission tomography imaging in dementia. Br J Radiol 2007;80(Spec No 2):S160–S167.
6. Ishii K. Clinical application of positron emission tomography for diagnosis of dementia. Ann Nucl Med 2002;16(8):515–525.
7. Matsunari I, Samuraki M, Chen WP, et al. Comparison of 18F-FDG PET and optimized voxel-based morphometry for detection of Alzheimer's disease: aging effect on diagnostic performance. J Nucl Med 2007;48(12):1961–1970.
8. Meltzer CC, Zubieta JK, Brandt J, Tune LE, Mayberg HS, Frost JJ. Regional hypometabolism in Alzheimer's disease as measured by positron emission tomography after correction for effects of partial volume averaging. Neurology 1996;47(2):454–461.
9. Perneczky R, Diehl-Schmid J, Drzezga A, Kurz A. Brain reserve capacity in frontotemporal dementia: a voxel-based 18F-FDG PET study. Eur J Nucl Med Mol Imaging 2007;34(7):1082–1087.
10. Perneczky R, Haussermann P, Diehl-Schmid J, et al. Metabolic correlates of brain reserve in dementia with Lewy bodies: an FDG PET study. Dement Geriatr Cogn Disord 2007;23(6):416–422.
11. Perneczky R, Häussermann P, Drzezga A, et al. Fluoro-deoxy-glucose positron emission tomography correlates of impaired activities of daily living in dementia with Lewy bodies: implications for cognitive reserve. Am J Geriatr Psychiatry 2009;17(3):188–195.
12. Dolan RJ, Bench CJ, Brown RG, Scott LC, Friston KJ, Frackowiak RS. Regional cerebral blood flow abnormalities in depressed patients with cognitive impairment. J Neurol Neurosurg Psychiatry 1992;55(9):768–773.
13. Rasgon NL, Kenna HA, Geist C, Small G, Silverman D. Cerebral metabolic patterns in untreated postmenopausal women with major depressive disorder. Psychiatry Res 2008;164(1):77–80.
14. Kawasaki K, Ishii K, Saito Y, Oda K, Kimura Y, Ishiwata K. Influence of mild hyperglycemia on cerebral FDG distribution patterns calculated by statistical parametric mapping. Ann Nucl Med 2008;22(3):191–200.
15. Hosaka K, Ishii K, Sakamoto S, et al. Validation of anatomical standardization of FDG PET images of normal brain: comparison of SPM and NEUROSTAT. Eur J Nucl Med Mol Imaging 2005;32(1):92–97.
16. Minoshima S, Giordani B, Berent S, Frey KA, Foster NL, Kuhl DE. Metabolic reduction in the posterior cingulate cortex in very early Alzheimer's disease. Ann Neurol 1997;42(1):85–94.
17. Buchert R, Wilke F, Chakrabarti B, et al. Adjusted scaling of FDG positron emission tomography images for statistical evaluation in patients with suspected Alzheimer's disease. J Neuroimaging 2005;15(4):348–355.
18. Yakushev I, Landvogt C, Buchholz HG, et al. Choice of reference area in studies of Alzheimer's disease using positron emission tomography with fluorodeoxyglucose-F18. Psychiatry Res 2008;164(2):143–153.
19. Choo IH, Lee DY, Youn JC, et al. Topographic patterns of brain functional impairment progression according to clinical severity staging in 116 Alzheimer disease patients: FDG-PET study. Alzheimer Dis Assoc Disord 2007;21(2):77–84.
20. Del Sole A, Clerici F, Chiti A, et al. Individual cerebral metabolic deficits in Alzheimer's disease and amnestic mild cognitive impairment: an FDG PET study. Eur J Nucl Med Mol Imaging 2008;35(7):1357–1366.
21. Hirono N, Hashimoto M, Ishii K, Kazui H, Mori E. One-year change in cerebral glucose metabolism in patients with Alzheimer's disease. J Neuropsychiatry Clin Neurosci 2004;16(4):488–492.
22. Jagust W, Reed B, Mungas D, Ellis W, Decarli C. What does fluorodeoxyglucose PET imaging add to a clinical diagnosis of dementia? Neurology 2007; 69(9):871–877.
23. Langbaum JB, Chen K, Lee W, et al. Categorical and correlational analyses of baseline fluorodeoxyglucose positron emission tomography images from the Alzheimer's Disease Neuroimaging Initiative (ADNI). Neuroimage 2009;45(4):1107–1116.
24. McMurtray AM, Licht E, Yeo T, Krisztal E, Saul RE, Mendez MF. Positron emission tomography facilitates diagnosis of early-onset Alzheimer's disease. Eur Neurol 2008;59(1-2):31–37.
25. Ishii K, Kono AK, Sasaki H, et al. Fully automatic diagnostic system for early- and late-onset mild Alzheimer's disease using FDG PET and 3D-SSP. Eur J Nucl Med Mol Imaging 2006;33(5):575–583.
26. Patterson JC, Lilien DL, Takalkar A, Kelley RE, Minagar A. Potential value of quantitative analysis

of cerebral PET in early cognitive decline. Am J Alzheimers Dis Other Demen 2008;23(6):586–592.
27. Gilman S, Koeppe RA, Little R, et al. Differentiation of Alzheimer's disease from dementia with Lewy bodies utilizing positron emission tomography with [18F]fluorodeoxyglucose and neuropsychological testing. Exp Neurol 2005;191(suppl 1):S95–S103.
28. Imamura T, Ishii K, Sasaki M, et al. Regional cerebral glucose metabolism in dementia with Lewy bodies and Alzheimer's disease: a comparative study using positron emission tomography. Neurosci Lett 1997;235(1-2):49–52.
29. Kono AK, Ishii K, Sofue K, Miyamoto N, Sakamoto S, Mori E. Fully automatic differential diagnosis system for dementia with Lewy bodies and Alzheimer's disease using FDG-PET and 3D-SSP. Eur J Nucl Med Mol Imaging 2007;34(9):1490–1497.
30. Minoshima S, Foster NL, Petrie EC, Albin RL, Frey KA, Kuhl DE. Neuroimaging in dementia with Lewy bodies: metabolism, neurochemistry, and morphology. J Geriatr Psychiatry Neurol 2002; 15(4):200–209.
31. Okamura N, Arai H, Higuchi M, et al. [18F]FDG-PET study in dementia with Lewy bodies and Alzheimer's disease. Prog Neuropsychopharmacol Biol Psychiatry 2001;25(2):447–456.
32. Colloby S, O'Brien J. Functional imaging in Parkinson's disease and dementia with Lewy bodies. J Geriatr Psychiatry Neurol 2004;17(3):158–163.
33. Higuchi M, Tashiro M, Arai H, et al. Glucose hypometabolism and neuropathological correlates in brains of dementia with Lewy bodies. Exp Neurol 2000;162(2):247–256.
34. Ishii K, Hosaka K, Mori T, Mori E. Comparison of FDG-PET and IMP-SPECT in patients with dementia with Lewy bodies. Ann Nucl Med 2004; 18(5):447–451.
35. Cordery RJ, Tyrrell PJ, Lantos PL, Rossor MN. Dementia with Lewy bodies studied with positron emission tomography. Arch Neurol 2001;58(3): 505–508.
36. Imamura T, Ishii K, Hirono N, et al. Occipital glucose metabolism in dementia with lewy bodies with and without Parkinsonism: a study using positron emission tomography. Dement Geriatr Cogn Disord 2001;12(3):194–197.
37. Perneczky R, Drzezga A, Boecker H, Förstl H, Kurz A, Häussermann P. Cerebral metabolic dysfunction in patients with dementia with Lewy bodies and visual hallucinations. Dement Geriatr Cogn Disord 2008;25(6):531–538.
38. Yong SW, Yoon JK, An YS, Lee PH. A comparison of cerebral glucose metabolism in Parkinson's disease, Parkinson's disease dementia and dementia with Lewy bodies. Eur J Neurol 2007;14(12): 1357–1362.
39. Foster NL. Validating FDG-PET as a biomarker for frontotemporal dementia. Exp Neurol 2003; 184(suppl 1):S2–S8.
40. Foster NL, Wang AY, Tasdizen T, Fletcher PT, Hoffman JM, Koeppe RA. Realizing the potential of positron emission tomography with 18F-fluorodeoxyglucose to improve the treatment of Alzheimer's disease. Alzheimers Dement 2008;4 (1 suppl 1):S29–S36.
41. Diehl J, Grimmer T, Drzezga A, Riemenschneider M, Förstl H, Kurz A. Cerebral metabolic patterns at early stages of frontotemporal dementia and semantic dementia: a PET study. Neurobiol Aging 2004;25(8):1051–1056.
42. Diehl-Schmid J, Grimmer T, Drzezga A, et al. Decline of cerebral glucose metabolism in frontotemporal dementia: a longitudinal 18F-FDG-PET study. Neurobiol Aging 2007;28(1):42–50.
43. Foster NL, Heidebrink JL, Clark CM, et al. FDG-PET improves accuracy in distinguishing frontotemporal dementia and Alzheimer's disease. Brain 2007;130(pt 10):2616–2635.
44. Grimmer T, Diehl J, Drzezga A, Förstl H, Kurz A. Region-specific decline of cerebral glucose metabolism in patients with frontotemporal dementia: a prospective 18F-FDG-PET study. Dement Geriatr Cogn Disord 2004;18(1):32–36.
45. Ibach B, Poljansky S, Marienhagen J, Sommer M, Männer P, Hajak G. Contrasting metabolic impairment in frontotemporal degeneration and early onset Alzheimer's disease. Neuroimage 2004;23(2): 739–743.
46. Jeong Y, Cho SS, Park JM, et al. 18F-FDG PET findings in frontotemporal dementia: an SPM analysis of 29 patients. J Nucl Med 2005;46(2):233–239.
47. Kanda T, Ishii K, Uemura T, et al. Comparison of grey matter and metabolic reductions in frontotemporal dementia using FDG-PET and voxel-based morphometric MR studies. Eur J Nucl Med Mol Imaging 2008;35(12):2227–2234.
48. Black S, Gao F, Bilbao J. Understanding white matter disease: imaging-pathological correlations in vascular cognitive impairment. Stroke 2009;40 (3 suppl):S48–S52.
49. Doyle CA, Slater P. Application of [3H]L-N(G)-nitro-arginine labelling to measure cerebellar nitric oxide synthase in patients with schizophrenia. Neurosci Lett 1995;202(1-2):49–52.
50. Kerrouche N, Herholz K, Mielke R, Holthoff V, Baron JC. 18FDG PET in vascular dementia: differentiation from Alzheimer's disease using voxel-based multivariate analysis. J Cereb Blood Flow Metab 2006;26(9):1213–1221.
51. Kuczynski B, Reed B, Mungas D, Weiner M, Chui HC, Jagust W. Cognitive and anatomic contributions of metabolic decline in Alzheimer disease and cerebrovascular disease. Arch Neurol 2008;65 (5):650–655.
52. Mielke R, Heiss WD. Positron emission tomography for diagnosis of Alzheimer's disease and vascular dementia. J Neural Transm Suppl 1998;53:237–250.
53. De Reuck J, Leys D, De Keyser J. Is positron emission tomography useful in stroke? Acta Neurol Belg 1997;97(3):168–171.
54. Duara R, Barker W, Loewenstein D, Pascal S, Bowen B. Sensitivity and specificity of positron emission tomography and magnetic resonance imaging studies in Alzheimer's disease and multi-infarct dementia. Eur Neurol 1989;29(suppl 3):9–15.
55. Meguro K, Doi C, Ueda M, et al. Decreased cerebral glucose metabolism associated with mental deterioration in multi-infarct dementia. Neuroradiology 1991;33(4):305–309.
56. Sultzer DL, Mahler ME, Cummings JL, Van Gorp WG, Hinkin CH, Brown C. Cortical abnormalities associated with subcortical lesions in vascular dementia: clinical and position emission tomographic findings. Arch Neurol 1995;52(8):773–780.
57. Tanaka M, Okamoto K, Hirai S. Cerebral blood flow and oxygen metabolism in vascular dementia evaluated by positron emission tomography: importance

of frontal lobe hypoperfusion and hypometabolism. Ann N Y Acad Sci 2002;977:135–140.
58. Tullberg M, Fletcher E, DeCarli C, et al. White matter lesions impair frontal lobe function regardless of their location. Neurology 2004;63(2):246–253.
59. Kotagal V, Lorincz MT, Bohnen NI. A frontotemporal dementia-like syndrome mimicking postpartum depression detected by 18F fluorodeoxyglucose positron emission tomography. Clin Nucl Med 2012;37(9):e223–e224.
60. Arlt S, Brassen S, Jahn H, et al. Association between FDG uptake, CSF biomarkers and cognitive performance in patients with probable Alzheimer's disease. Eur J Nucl Med Mol Imaging 2009;36(7):1090–1100.
61. Vukovich R, Perneczky R, Drzezga A, Förstl H, Kurz A, Riemenschneider M. Brain metabolic correlates of cerebrospinal fluid beta-amyloid 42 and tau in Alzheimer's disease. Dement Geriatr Cogn Disord 2009;27(5):474–480.
62. Morbelli S, Piccardo A, Villavecchia G, et al. Mapping brain morphological and functional conversion patterns in amnestic MCI: a voxel-based MRI and FDG-PET study. Eur J Nucl Med Mol Imaging 2010;37(1):36–45.
63. Mosconi L, Tsui WH, Herholz K, et al. Multicenter standardized 18F-FDG PET diagnosis of mild cognitive impairment, Alzheimer's disease, and other dementias. J Nucl Med 2008;49(3):390–398.
64. Yuan Y, Gu ZX, Wei WS. Fluorodeoxyglucose-positron-emission tomography, single-photon emission tomography, and structural MR imaging for prediction of rapid conversion to Alzheimer disease in patients with mild cognitive impairment: a meta-analysis. AJNR Am J Neuroradiol 2009;30(2):404–410.
65. Chételat G, Desgranges B, Landeau B, et al. Direct voxel-based comparison between grey matter hypometabolism and atrophy in Alzheimer's disease. Brain 2008;131(pt 1):60–71.
66. Minoshima S, Cross DJ, Foster NL, Henry TR, Kuhl DE. Discordance between traditional pathologic and energy metabolic changes in very early Alzheimer's disease: pathophysiological implications. Ann N Y Acad Sci 1999;893:350–352.
67. Baron JC, Lebrun-Grandie P, Collard P, Crouzel C, Mestelan G, Bousser MG. Noninvasive measurement of blood flow, oxygen consumption, and glucose utilization in the same brain regions in man by positron emission tomography: concise communication. J Nucl Med 1982;23(5):391–399.
68. Herholz K. Perfusion SPECT and FDG-PET. Int Psychogeriatr 2011;23(suppl 2):S25–S31.
69. Markiewicz PJ, Matthews JC, Declerck J, Herholz K. Robustness of multivariate image analysis assessed by resampling techniques and applied to FDG-PET scans of patients with Alzheimer's disease. Neuroimage 2009;46(2):472–485.
70. Markiewicz PJ, Matthews JC, Declerck J, Herholz K; Alzheimer's Disease Neuroimaging Initiative (ADNI). Verification of predicted robustness and accuracy of multivariate analysis. Neuroimage 2011;56(3):1382–1385.
71. Zahn R, Garrard P, Talazko J, et al. Patterns of regional brain hypometabolism associated with knowledge of semantic features and categories in Alzheimer's disease. J Cogn Neurosci 2006;18(12):2138–2151.
72. Foster NL, VanDerSpek AF, Aldrich MS, et al. The effect of diazepam sedation on cerebral glucose metabolism in Alzheimer's disease as measured using positron emission tomography. J Cereb Blood Flow Metab 1987;7(4):415–420.
73. Wang BW, Lu E, Mackenzie IR, et al. Multiple pathologies are common in Alzheimer patients in clinical trials. Can J Neurol Sci 2012;39(5):592–599.
74. Alladi S, Xuereb J, Bak T, et al. Focal cortical presentations of Alzheimer's disease. Brain 2007;130(pt 10):2636–2645.
75. McKhann GM, Knopman DS, Chertkow H, et al. The diagnosis of dementia due to Alzheimer's disease: recommendations from the National Institute on Aging-Alzheimer's Association workgroups on diagnostic guidelines for Alzheimer's disease. Alzheimers Dement 2011;7(3):263–269.
76. Burke JF, Albin RL, Koeppe RA, et al. Assessment of mild dementia with amyloid and dopamine terminal positron emission tomography. Brain 2011;134(pt 6):1647–1657.

Brain PET in Suspected Dementia: Patterns of Altered FDG Metabolism

Richard K. J. Brown, MD • Nicolaas I. Bohnen, MD, PhD • Ka Kit Wong, MBBS • Satoshi Minoshima, MD, PhD • Kirk A. Frey, MD, PhD

RadioGraphics 2014; 34:684–701 • **Published online** 10.1148/rg.343135065 • **Content Codes:** MI NM NR

Page 685
Histopathologic analysis is the standard of reference for the diagnosis of Alzheimer disease.

Page 685
Elevated glucose levels can interfere with FDG uptake in the brain.

Page 685
The uptake of FDG when the patient's eyes are closed may cause hypometabolism in the occipital lobe, possibly leading to a misdiagnosis of DLB.

Page 688
This involvement of the occipital lobes is compatible with the clinical diagnosis of DLB.

Page 689
Classic FTD is characterized by hypometabolism in the frontal and anterior temporal lobes with involvement of the anterior cingulate gyrus.